Synthesis of Triangular and Tetrahedral Heteronuclear Metal Clusters Using Hydride Complexes of Cyclopentadienylrhodium and -ruthenium as the Precursors

Takayuki Nakajima and Isao Shimizu*

Department of Applied Chemistry, School of Science and Engineering, Waseda University, Ookubo 3-4-1, Shinjuku-ku, Tokyo 169, Japan

Kimiko Kobayashi and Yasuo Wakatsuki*

The Institute of Physical and Chemical Research (RIKEN), Hirosawa 2-1, Wako-shi, Saitama 351-0198, Japan

Received September 2, 1997

Photochemical and/or thermal reactions of $Cp^*Rh(H)_2(SiEt_3)_2$ ($Cp^* = \eta^5$-C_5Me_5) with the dimeric metal complexes $[CpNi(CO)]_2$ ($Cp = \eta^5$-C_5H_5), $[CpCo(NO)]_2$, $[CpRu(CO)_2]_2$, and $[CpFe(CO)_2]_2$ yielded the trinuclear complexes $(Cp^*Rh)(CpNi)_2(CO)_2$ (**3**), $(Cp^*Rh)(CpCo)_2(NO)_2$ (**4**), $(Cp^*Rh)(CpM)_2(CO)_4$ (**5a**, M = Ru; **5b**, M = Fe), respectively, while the reaction with $[CpMo(CO)_2]_2$ gave the tetranuclear unsaturated complex $(Cp^*Rh)_2(CpMo)_2(CO)_4$ (**6**) in good to moderate yields. Similarly, $[Cp^*Ru]_2(\mu$-$H)_4$ reacted with $[CpNi(CO)]_2$, $CpCo(CO)_2$, and $[CpFe(CO)_2]_2$ to give tetrahedral $(Cp^*Ru)_2(CpNi)_2(CO)_2$ (**7**), triangular $(Cp^*Ru)_2(CpCo)(CO)_4$ (**8**), and tetrahedral $(Cp^*Ru)_2(CpFe)_2(CO)_4$ (**9**) complexes, respectively. The mixed-metal clusters **3**, **4**, **5a**, and **6**−**9** have been structurally characterized by single-crystal X-ray diffraction.

Introduction

Heterometallic clusters have attracted considerable interest in many respects.[1] One example is their application as precursors for high mixed-metal dispersions, which may be useful as heterogeneous catalysts[2] or nanoscale materials[2−4] of discrete metal composition. Even though many heterometallic cluster complexes have been prepared, their number and combinations of metals are not satisfactory, particularly from the viewpoint of the above-mentioned applications. In the search for an efficient route to new heterometallic clusters, we have found that hydride complexes of rhodium and ruthenium, $Cp^*Rh(H)_2(SiEt_3)_2$ (**1**; $Cp^* = \eta^5$-C_5Me_5) and $[Cp^*Ru]_2(\mu$-$H)_4$ (**2**), are good precursors to heteronuclear metal clusters containing the Cp*Rh or Cp*Ru fragment. This is an extension of the strategy described in our previous report that "Cp_2M" (M = Mo, W) generated on photolysis of Cp_2MH_2 is smoothly incorporated into dimeric metal complexes to form new heterometallic bonds.[5] The usefulness of **1** and **2** as precursors has been demonstrated by their facile photochemical or thermal reactions with appropriate mono- and dinuclear cyclopentadienylmetal complexes (Scheme 1). Seven novel triangular and tetrahedral mixed-metal clusters thus prepared have been characterized by single-crystal X-ray analysis. All the novel mixed-metal cluster complexes reported here are readily soluble in common organic solvents, and most of them are sublimable: these properties may be important when considering the application of these complexes as sources for heterometal deposition.

Results and Discussion

Reactions of $Cp^*Rh(H)_2(SiEt_3)_2$ with $[CpNi(CO)]_2$ and $[CpCo(NO)]_2$. The easily accessible rhodium hydride complex $Cp^*Rh(H)_2(SiEt_3)_2$ (**1**) reacted slowly but cleanly with an equimolar amount of $[CpNi(CO)]_2$ in THF when irradiated with a high-pressure mercury lamp. The reaction was conveniently monitored by sampling a small portion and measuring its ^{1}H NMR signals. The initially red solution turned dark green, with a small amount of dark red precipitate forming gradually. After 4 days of irradiation, the mixture was worked up on a column chromatograph to give green crystals with the composition $(Cp^*Rh)(CpNi)_2(CO)_2$ (**3**) in 41% yield. The same cluster complex was obtained in 35% yield when **1** and the nickel dimer in toluene were heated at 80 °C for 72 h. A closely related complex, $(CpRh)(CpNi)_2(CO)_2$, has been prepared in very low yields (3.5−4.0%) by the reaction of $CpRh(C_2H_4)_2$ with $[CpNi(CO)]_2$, but its structural characterization has not been reported.[6]

The IR spectrum in THF showed a single ν(CO) band at 1732 cm^{-1}, indicating that the two CO ligands are probably in the μ_3 coordination mode. Equivalence of

(1) *Comprehensive Organometallic Chemistry*; Wilkinson, G., Stone, F. G. A., Abel, E. W., Eds.; Pergamon: New York, 1995; Vol. 10.
(2) Gates, B. C. *Chem. Rev.* **1995**, *95*, 511.
(3) Choi, K. M.; Shea, K. J. *J. Am. Chem. Soc.* **1994**, *116*, 9052.
(4) Lewis, L. N. *Chem. Rev.* **1993**, *93*, 2693.
(5) Nakajima, T.; Mise, T.; Shimizu, I.; Wakatsuki, Y. *Organometallics* **1995**, *14*, 5598.
(6) Walther, B.; Scheer, M.; Böttcher, H. C. *Inorg. Chim. Acta* **1989**, *156*, 285.

S0276-7333(97)00772-3 CCC: $15.00
Publication on Web 01/19/1998

Scheme 1

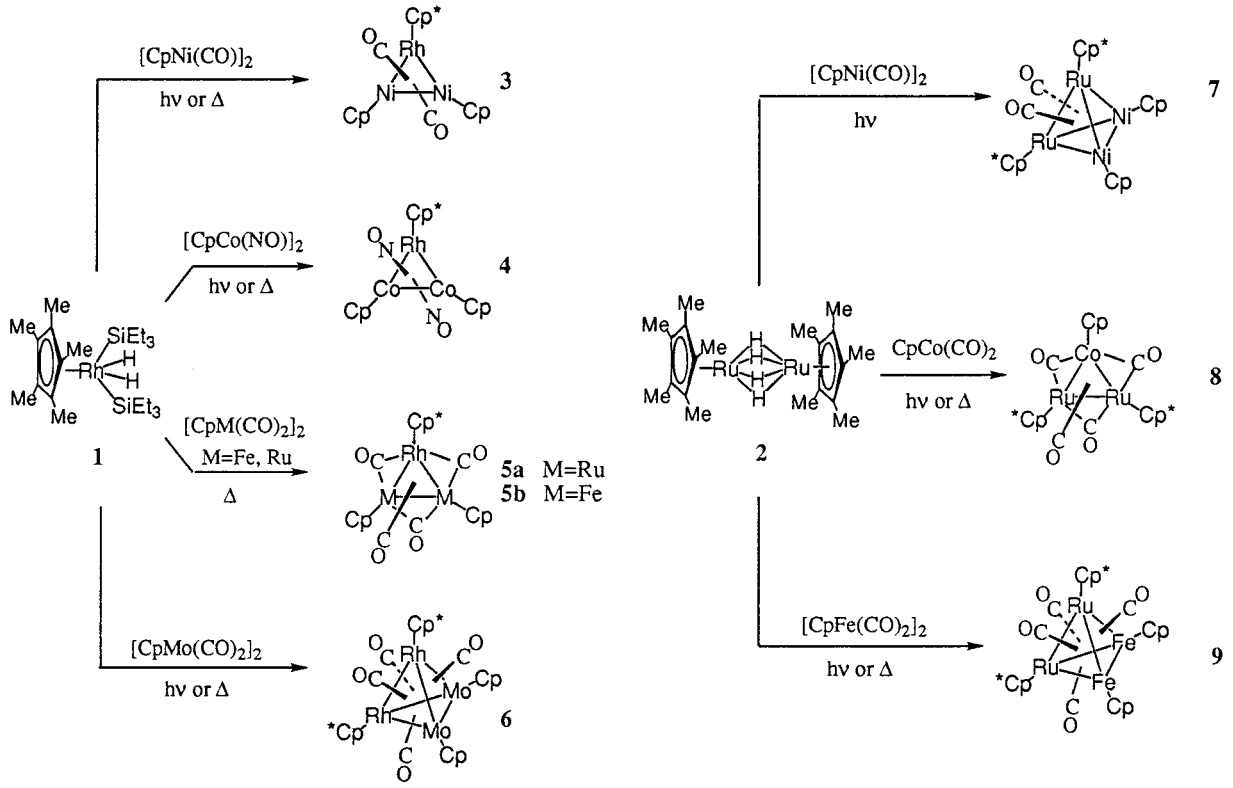

Table 1. NMR and IR Data for Complexes 3−9

	^{1}H NMR (ppm)[a]		^{13}C NMR (ppm)[b]					IR (THF, cm^{-1})
	Cp	Cp*	μ_3-CO	μ_2-CO	Cp*	Cp	Me	ν(CO) (ν(NO))
3	5.13	1.64	237.6[c]		102.7[d]	92.1	9.8	1732 vs
4	4.56	1.51			97.7[e]	86.4	9.1	(1393 vs, 1372 vs)
5a	4.94	1.63	252.3[f]	243.9, 234.7[g]	106.5[h]	93.4	8.4	1831 vs, 1783 s, 1773 s, 1660 s
5b	4.42	1.57	277.4[i]	267.3, 246.3[j]	107.7[k]	92.1	8.5	1829 vs, 1783 s, 1772 s, 1663 s
6	5.38	1.47	266.61,[l] 255.0,[m] 254.9[m]	104.1,[n] 104.0[n]	98.3	6.9	2018 w, 1954 m, 1875 w, 1773 vw, 1761 vw, 1701 m, 1654 vs	
7	4.82	2.01	not measured[o]					1647 vs
8	4.63	1.63	269.1	250.3, 249.2	102.9	93.0	8.6	1821vs, 1734 s, 1759 s, 1660 s
9	4.44	1.65	281.1, 268.0		105.3	98.2	8.7	1634 vs

[a] **3**−**9**: in C_6D_6. [b] **5a**: in $CDCl_3$; **3**, **4**, **5b** in C_6D_6; **8**, **9** in $C_6D_5CD_3$. [c] Doublet, J(RhC) = 43.3 Hz. [d] Doublet, J(RhC) = 5.5 Hz. [e] Doublet, J(RhC) = 6.9 Hz. [f] Doublet, J(RhC) = 29.7 Hz. [g] Doublet, J(RhC) = 32.1 Hz. [h] Doublet, J(RhC) = 6.0 Hz. [i] Doublet, J(RhC) = 29.2 Hz. [j] Doublet, J(RhC) = 33.9 Hz. [k] Doublet, J(RhC) = 4.7 Hz. [l] Triplet, J(RhC) = 22.6 Hz. [m] Doublet, J(RhC) = 8.7 Hz. [n] Doublet, J(RhC) = 2.5 Hz. [o] Complex **7** decomposes gradually in solution.

the two CO and also the two Cp ligands was obvious from NMR spectra (Table 1). The solid-state structure of **3** has been determined by single-crystal X-ray diffraction as shown in Figure 1, which was consistent with the spectra in solution. Important bond lengths and angles are given in Table 2. The Ni−Ni bond length was 2.339(1) Å and, as expected, was significantly longer than that reported for the cobalt analog of **3**, (Cp*Co)-$(CpNi)_2(CO)_2$ (2.326(2) Å).[7]

A similar reaction of **1** with $[CpCo(NO)]_2$, either photochemically or thermally, afforded dark red crystals of the composition $(Cp^*Rh)(CpCo)_2(NO)_2$ (**4**) in 41% (photochemical) or 83% (thermal) yield. The X-ray structure of **4** is shown in Figure 2, while selected bond lengths and angles are listed in Table 3. The solid-state structure of the analogous triangular frame, but with a 46-electron configuration, $(Cp^*Rh)(CpCo)_2(CO)_2$, has been reported to have two Rh−Co and one Co−Co distance of 2.433(1), 2.431(1), and 2.426(1) Å, respectively.[8] The saturated 48-electron cluster **4** has considerably longer Rh−Co distances of 2.516(1) and 2.521-(1) Å and a slightly longer Co−Co distance of 2.434(2) Å, indicating that the additional 2 electrons brought in by NO ligands in place of the two CO's have populated an orbital with Rh−Co antibonding character. The bonding scheme in $(CpRh)_3(CO)_2$ with a LUMO of metal−metal antibonding character has been reported.[9] The two CO ligands in $(Cp^*Rh)(CpCo)_2(CO)_2$ are Co−Co edge bridging (Rh−C(CO) = 2.32 Å), but in **4** the two NO's are capping the triangular metal plane, the N−metal distances being much more averaged (e.g. Rh−N = 2.00 Å).

(7) Byers, L. R.; Uchtman, V. A.; Dahl, L. F. *J. Am. Chem. Soc.* **1981**, *103*, 1942.

(8) Barnes, C. E.; Dial, M. R.; Orvis, J. A.; Staley, D. L.; Rheingold, A. L. *Organometallics* **1990**, *9*, 1021.

(9) Pinhaus, A. R.; Albright, T. A.; Hofmann, P.; Hoffmann, R. *Helv. Chim. Acta* **1980**, *63*, 29.

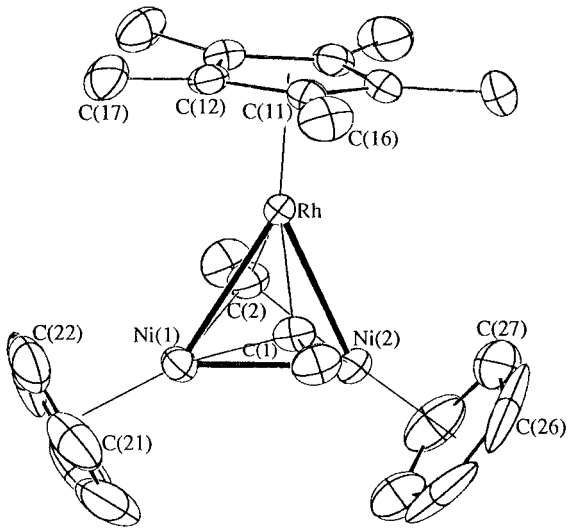

Figure 1. Molecular structure and numbering scheme for **3** drawn at the 30% probability level.

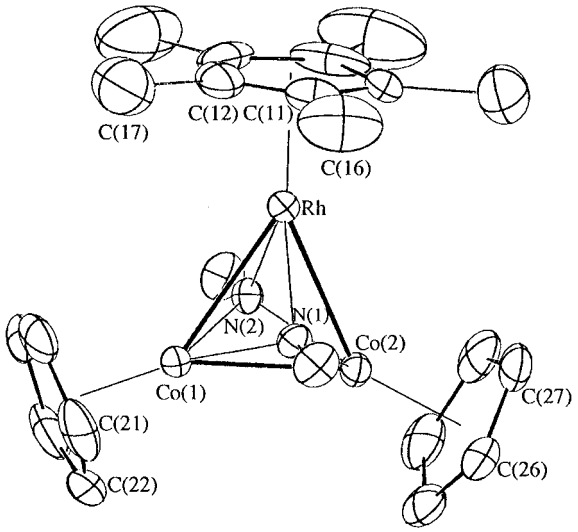

Figure 2. Molecular structure and numbering scheme for **4** drawn at the 30% probability level.

Table 2. Selected Bond Lengths (Å) and Angles (deg) for 3

	Bond Lengths		
Rh−Ni(1)	2.486(1)	Rh−Ni(2)	2.489(1)
Ni(1)−Ni(2)	2.339(1)		
Rh−C(1)	1.975(7)	Rh−C(2)	1.987(8)
Ni(1)−C(1)	1.994(7)	Ni(1)−C(2)	2.037(8)
Ni(2)−C(1)	2.058(7)	Ni(2)−C(2)	1.981(7)
C(1)−O(1)	1.179(9)	C(2)−O(2)	1.184(10)
	Bond Angles		
Ni(1)−Rh−Ni(2)	56.10(3)	Rh−Ni(1)−Ni(2)	62.02(3)
Rh−Ni(2)−Ni(1)	61.88(3)		
Rh−C(1)−Ni(1)	77.6(3)	Rh−C(2)−Ni(1)	76.3(3)
Rh−C(1)−Ni(2)	76.2(3)	Rh−C(2)−Ni(2)	77.7(3)
Ni(1)−C(1)−Ni(2)	70.5(2)	Ni(1)−C(2)−Ni(2)	71.2(3)
Rh−C(1)−O(1)	141.3(6)	Rh−C(2)−O(2)	139.6(6)
Ni(1)−C(1)−O(1)	133.0(6)	Ni(1)−C(2)−O(2)	132.6(7)
Ni(2)−C(1)−O(1)	130.7(5)	Ni(2)−C(2)−O(2)	132.7(6)

Reactions of 1 with $[CpM(CO)_2]_2$ (M = Ru, Fe). The rhodium species **1** reacted with $[CpRu(CO)_2]_2$ in toluene at 70 °C, yielding fine green crystals of the formula $(Cp^*Rh)(CpRu)_2(CO)_4$ (**5a**) in 38% yield. The IR spectrum indicated the presence of μ_3-CO (ν(CO) 1660 cm^{-1}) and μ_2-CO ligands (Table 1). The ^{13}C NMR spectrum of the CO region showed that three of the four CO ligands (252.3 and 234.7 ppm) were bonded to Rh, Rh−C coupling being observed. The solid-state structure (Figure 3, Table 4) was consistent with the solution spectroscopy, which had one CO capping the triangular plane and three CO ligands bridging the three metal−metal edges. The three μ_2-CO groups are tilted toward the other side of the μ_3-CO ligand with respect to the triangular metal plane, and the dihedral angles between

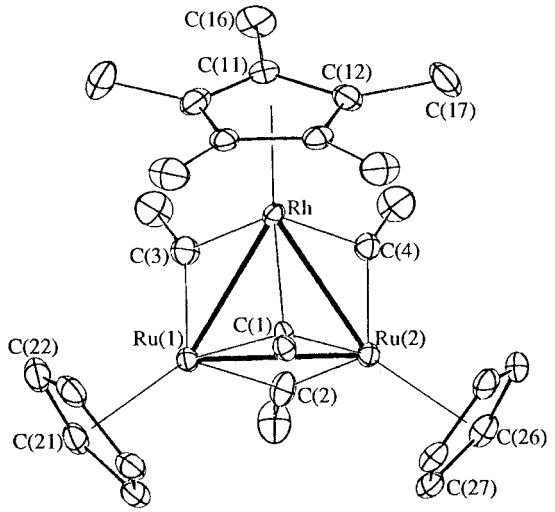

Figure 3. Molecular structure and numbering scheme for **5a** drawn at the 30% probability level.

Table 3. Selected Bond Lengths (Å) and Angles (deg) for 4

	Bond Lengths		
Rh−Co(1)	2.516(1)	Rh−Co(2)	2.521(1)
Co(1)−Co(2)	2.434(2)		
Rh−N(1)	1.999(7)	Rh−C(2)	1.989(6)
Co(1)−N(1)	1.857(7)	Co(1)−N(2)	1.864(6)
Co(2)−N(1)	1.867(6)	Co(2)−N(2)	1.859(8)
N(1)−O(1)	1.235(9)	N(2)−O(2)	1.246(9)
	Bond Angles		
Co(1)−Rh−Co(2)	57.80(4)	Rh−Co(1)−Co(2)	61.20(4)
Rh−Co(2)−Co(1)	61.00(4)		
Rh−N(1)−Co(1)	81.4(3)	Rh−N(2)−Co(1)	81.5(2)
Rh−N(1)−Co(2)	81.3(2)	Rh−N(2)−Co(2)	81.8(3)
Co(1)−N(1)−Co(2)	81.7(2)	Co(1)−N(2)−Co(2)	81.7(3)
Rh−N(1)−O(1)	129.9(6)	Rh−N(2)−O(2)	130.3(6)
Co(1)−N(1)−O(1)	130.8(5)	Co(1)−N(2)−O(2)	130.7(6)
Co(2)−N(1)−O(1)	132.6(6)	Co(2)−N(2)−O(2)	131.9(6)

Table 4. Selected Bond Lengths (Å) and Angles (deg) for 5a

	Bond Lengths		
Rh−Ru(1)	2.715(3)	Rh−C(1)	2.104(9)
Rh−Ru(2)	2.708(3)	Rh−C(3)	2.108(13)
Ru(1)−Ru(2)	2.721(1)	Rh−C(4)	2.140(12)
Ru(1)−C(1)	2.158(29)	Ru(2)−C(1)	2.007(27)
Ru(1)−C(2)	2.066(39)	Ru(2)−C(2)	1.998(37)
Ru(1)−C(3)	1.952(12)	Ru(2)−C(4)	1.950(11)
C(1)−O(1)	1.193(12)	C(2)−O(2)	1.188(16)
C(3)−O(3)	1.182(16)	C(4)−O(4)	1.174(15)
	Bond Angles		
Ru(1)−Rh−Ru(2)	60.22(3)	C(1)−Rh−C(3)	96.8(8)
Rh−Ru(1)−Ru(2)	59.7(1)	C(1)−Rh−C(4)	92.8(8)
Rh−Ru(2)−Ru(1)	60.0(1)	C(3)−Rh−C(4)	80.3(5)
C(1)−Ru(1)−C(2)	93.6(14)	C(1)−Ru(2)−C(2)	100.6(15)
C(1)−Ru(1)−C(3)	100.0(5)	C(1)−Ru(2)−C(4)	102.0(5)
C(2)−Ru(1)−C(3)	83.7(5)	C(2)−Ru(2)−C(4)	83.5(5)
Rh−C(1)−Ru(1)	79.1(7)	Ru(1)−C(2)−Ru(2)	84.0(4)
Rh−C(1)−Ru(2)	82.4(6)	Rh−C(3)−Ru(1)	83.8(5)
Ru(1)−C(1)−Ru(2)	81.5(4)	Rh−C(4)−Ru(2)	82.8(4)

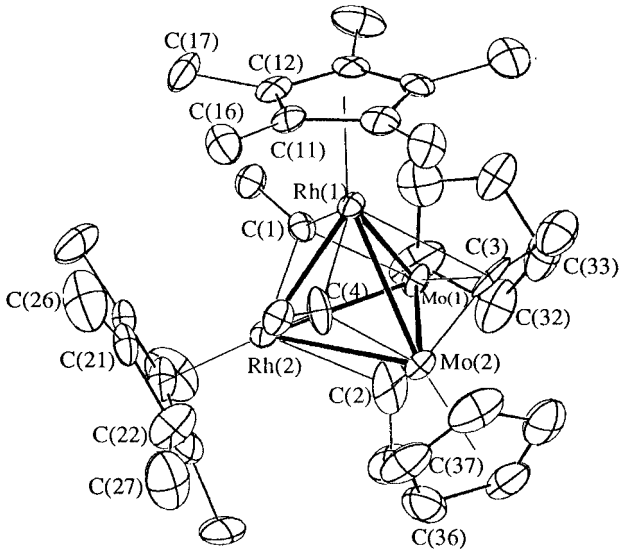

Figure 4. Molecular structure and numbering scheme for **6** drawn at the 30% probability level.

the planes Rh−Ru−Ru and $M^1-M^2-C(\mu_2\text{-CO})$ are 124 (Rh−Ru(1)), 118 (Rh−Ru(2)), and 118° (Ru−Ru). To avoid steric interactions with these tilted μ_2-CO groups, the Cp* is bent toward the other side of the triangular plane (dihedral angle Rh−Ru−Ru/Cp* 71°), while similar tiltings of Cp ligands have dihedral angles of 78° and 72°.

By using $[CpFe(CO)_2]_2$ in place of its Ru analog, a dark red solid of $(Cp^*Rh)(CpFe)_2(CO)_4$ (**5b**) was isolated in 53% yield. It shows IR and NMR spectra very similar to those of **5a** (Table 1). A complex closely related to **5b**, $(CpRh)(CpFe)_2(CO)_4$, has been prepared from $CpRh(C_2H_4)_2$ and $[CpFe(CO)_2]_2$ in a low yield (9%), though no crystal structure analysis has been reported.[6]

Photochemical reactions of **1** with $[CpM(CO)_2]_2$ (M = Ru, Fe) were not practical since they produced too many side products that were difficult to separate.

Reaction of 1 with $[CpMo(CO)_2]_2$. The unsaturated molybdenum dimer $[CpMo(CO)_2]_2$ reacted with 2 equiv of **1** under irradiation for 62 h. Subsequent workup of the reaction mixture on a column chromatograph gave a dark red crystalline solid with the formula $(Cp^*Rh)_2(CpMo)_2(CO)_4$ (**6**) in 24% yield. Recrystallization gave dark red plates. The same complex was obtained in better yield (58%) when the reaction was carried out thermally at 70 °C. Even when the reaction was performed in a 1:1 molar ratio, tetranuclear **6** was formed in lower yield while the expected trinuclear metal complex was not observed.

The number of valence electrons of **6** is 58, i.e. 2 fewer electrons than the total valence electrons expected for a saturated tetrahedral cluster complex. Probably because of that, **6** is much less stable on heating than the other cluster complexes described above: its toluene solution gradually decomposes at 80 °C.

The molecular structure of **6**, established by X-ray crystal analysis, is shown in Figure 4 with important bond lengths and angles as listed in Table 5. Though the unit cell has contained two independent units, structural parameters for only one of them are given in the table since the differences between the two are very small. The metal frame is distorted tetrahedral with triply bridging CO ligands capping the four planes. This

Table 5. Selected Bond Lengths (Å) and Angles (deg) for 6

Bond Lengths			
Rh(1)−Rh(2)	2.713(3)	Rh(2)−Mo(1)	2.728(3)
Rh(1)−Mo(1)	2.819(2)	Rh(2)−Mo(2)	2.829(3)
Rh(1)−Mo(2)	2.721(3)	Mo(1)−Mo(2)	2.709(3)
Rh(1)−C(1)	2.122(20)	Rh(2)−C(2)	2.460(22)
Rh(2)−C(1)	2.268(21)	Mo(1)−C(2)	2.336(23)
Mo(1)−C(1)	2.034(21)	Mo(2)−C(2)	1.981 (22)
Rh(1)−C(3)	2.440(23)	Rh(1)−C(4)	2.293(21)
Mo(1)−C(3)	1.951(22)	Rh(2)−C(4)	2.111(19)
Mo(2)−C(3)	2.368(23)	Mo(2)−C(4)	1.986(21)
C(1)−O(1)	1.210(25)	C(2)−O(2)	1.150(27)
C(3)−O(3)	1.201(28)	C(4)−O(4)	1.237(25)

Bond Angles			
Rh(2)−Rh(1)−Mo(1)	59.1(1)	Rh(1)−Rh(2)−Mo(1)	62.4(1)
Rh(2)−Rh(1)−Mo(2)	62.8(1)	Rh(1)−Rh(2)−Mo(2)	58.8(1)
Mo(1)−Rh(1)−Mo(2)	58.5(1)	Mo(1)−Rh(2)−Mo(2)	58.3(1)
Rh(1)−Mo(1)−Rh(2)	58.5(1)	Rh(1)−Mo(2)−Rh(2)	58.5(1)
Rh(1)−Mo(1)−Mo(2)	58.9(1)	Rh(1)−Mo(2)−Mo(1)	62.6(1)
Rh(2)−Mo(1)−Mo(2)	62.7(1)	Rh(2)−Mo(2)−Mo(1)	59.0(1)
C(1)−Rh(1)−C(3)	84.2(8)	C(1)−Rh(2)−C(2)	100.2(8)
C(1)−Rh(1)−C(4)	103.3(8)	C(1)−Rh(2)−C(4)	104.5(8)
C(3)−Rh(1)−C(4)	100.0(8)	C(2)−Rh(2)−C(4)	83.3(8)
C(1)−Mo(1)−C(2)	112.1(8)	C(2)−Mo(2)−C(3)	98.0(8)
C(1)−Mo(1)−C(3)	100.6(9)	C(2)−Mo(2)−C(4)	100.5(9)
C(2)−Mo(1)−C(3)	99.9(9)	C(3)−Mo(2)−C(4)	112.5(8)
Rh(1)−C(1)−Rh(2)	76.3(7)	Rh(2)−C(2)−Mo(1)	69.3(6)
Rh(1)−C(1)−Mo(1)	85.4(8)	Rh(2)−C(2)−Mo(2)	78.3(7)
Rh(2)−C(1)−Mo(1)	78.5(7)	Mo(1)−C(2)−M°(2)	77.3(8)
Rh(1)−C(3)−Mo(1)	79.0(8)	Rh(1)−C(4)−Rh(2)	75.9(7)
Rh(1)−C(3)−Mo(2)	68.9(6)	Rh(1)−C(4)−Mo(2)	78.6(7)
Mo(1)−C(3)−Mo(2)	77.0(8)	Rh(2)−C(4)−Mo(2)	87.3(8)

is a big contrast to the structure reported for a cobalt−molybdenum complex with similar composition $(Cp^*Co)_2(CpMo)_2(CO)_4$, where two Co−Mo bonds are broken and instead a μ_4-CO ligand is present.[10] In complex **6**, two of the four Rh−Mo bonds, Rh(1)−Mo(2) and Rh(2)−Mo(1), are ca. 0.1 Å shorter than the other two (Table 5), which leads to the distorted metal framework. The small but significant partial double-bond character of these two bonds may be explained by the unsaturation of valence electrons in this complex. The positions of the CO ligands are also significantly displaced from the ideal μ_3 coordination, and the metal−C(CO) distances range from 1.95(2) Å for Mo(1)−C(3) to 2.46(2) Å for Rh(2)−C(2).

The distortion of the cluster structure is noted in solution also: the ^{13}C NMR shows three resonances for the four CO ligands, while two peaks would have been expected if the cluster was electronically saturated and not deformed. Likewise, the two Cp* ligands are observed to be nonequivalent (Table 1). The IR spectrum in THF has altogether seven ν(CO) peaks, in the region 2018 (w) cm^{-1} to 1654 (vs) cm^{-1}, suggesting that the μ_3-CO ligands in **6** are fractional in terms of their positions within the coordinating triangular metal planes.

Reaction of $[Cp^*Ru]_2(\mu\text{-H})_4$ with $[CpNi(CO)]_2$. The dimeric ruthenium tetrahydride complex $[Cp^*Ru]_2(\mu\text{-H})_4$ (**2**) was found to react photochemically with an equimolar amount of $[CpNi(CO)]_2$, as monitored by ^1H NMR spectra of the reaction mixture. After irradiation for 35 h at room temperature, workup on a column chromatograph eventually gave dark red crystals of $(Cp^*Ru)_2(CpNi)_2(CO)_2$ (**7**) in 36% yield. In solution this

(10) Brun, P.; Dawkins, G. M.; Green, M.; Miles, A. D.; Orpen, A. G.; Stone, F. G. A. *J. Chem. Soc., Chem. Commun.* **1982**, 926.

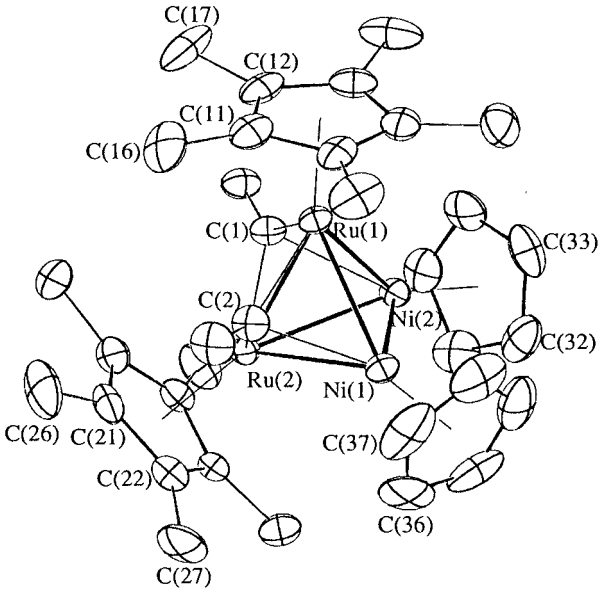

Figure 5. Molecular structure and numbering scheme for **7** drawn at the 30% probability level.

Table 6. Selected Bond Lengths (Å) and Angles (deg) for 7

Bond Lengths			
Ru(1)−Ru(2)	2.631(1)	Ru(2)−Ni(1)	2.555(1)
Ru(1)−Ni(1)	2.563(1)	Ru(2)−Ni(2)	2.569(1)
Ru(1)−Ni(2)	2.552(1)	Ni(1)−Ni(2)	2.497(1)
Ru(1)−C(1)	2.008(8)	Ru(1)−C(2)	2.041(9)
Ru(2)−C(1)	2.025(8)	Ru(2)−C(2)	2.042(9)
Ni(1)−C(1)	2.165(9)	Ni(2)−C(2)	2.177(10)
C(1)−O(1)	1.221(10)	C(2)−O(2)	1.212(11)

Bond Angles			
Ru(2)−Ru(1)−Ni(1)	58.93(3)	Ru(1)−Ru(2)−Ni(1)	59.22(3)
Ru(2)−Ru(1)−Ni(2)	59.40(3)	Ru(1)−Ru(2)−Ni(2)	58.78(3)
Ni(1)−Ru(1)−Ni(2)	58.44(4)	Ni(1)−Ru(2)−Ni(2)	58.33(4)
Ru(1)−Ni(1)−Ru(2)	61.85(3)	Ru(1)−Ni(2)−Ru(2)	61.82(3)
Ru(1)−Ni(1)−Ni(2)	60.56(4)	Ru(1)−Ni(2)−Ni(1)	61.01(4)
Ru(2)−Ni(1)−Ni(2)	61.10(4)	Ru(2)−Ni(2)−Nit1)	60.57(4)
C(1)−Ru(1)−C(2)	96.0(4)	C(1)−Ru(2)−C(2)	95.5(4)
Ru(1)−C(1)−Ru(2)	81.4(3)	Ru(1)−C(2)−Ru(2)	80.2(3)
Ru(1)−C(1)−Ni(1)	75.7(3)	Ru(1)−C(2)−Ni(2)	74.4(3)
Ru(2)−C(1)−Ni(1)	75.1(3)	Ru(2)−C(2)−Ni(2)	74.9(3)
Ru(1)−C(1)−O(1)	138.3(7)	Ru(1)−C(2)−O(2)	138.2(7)
Ru(2)−C(1)−O(1)	136.7(7)	Ru(2)−C(2)−O(2)	138.1(7)
Ni(1)−C(1)−O(1)	122.9(6)	Ni(2)−C(2)−O(2)	123.2(7)

compound is thermally unstable and slowly decomposes on standing under argon for a few days at moderate temperatures. Thermal preparation of **7** was, therefore, not feasible.

The molecular structure of **7** has been determined by X-ray analysis, as shown in Figure 5, and selected atom distances and angles are listed in Table 6. The unit cell contains three independent units, but only one of these is shown in Figure 5 and Table 6 since differences between the independent units are very small. The metal frame has a tetrahedral structure, and the Ni−Ni distance (2.497(1) Å) is considerably longer than that in triangular **3** (2.339(1) Å). The two CO ligands occupy the positions on the two Ru−Ru−Ni triangles. The mean Ru−C(CO) distance is 2.029 Å, while Ni−C(CO) distances are distinctively longer at 2.165(9) and 2.177(10) Å. The Ru−Ru−C(CO) plane and the C−O bond form a tilt angle of 167° for both CO groups, which is very close to the value observed in $(Cp^*Co)(CpCo)_2(CO)_2$, where an edge-bridging coordination mode of the CO's has been claimed.[8] These structural features of **7** imply that the two CO's are shifted toward edge bridging at Ru−Ru from the ideal face-capping coordination. The 18-electron rule on each metal atom in **7** would account for this trend and at the same time explains why the CO ligands are not located on the Ru−Ni−Ni faces. The IR spectrum, however, showed a single ν(CO) band at 1647 cm^{-1} in the typical region for a μ_3-CO ligand (Table 1).

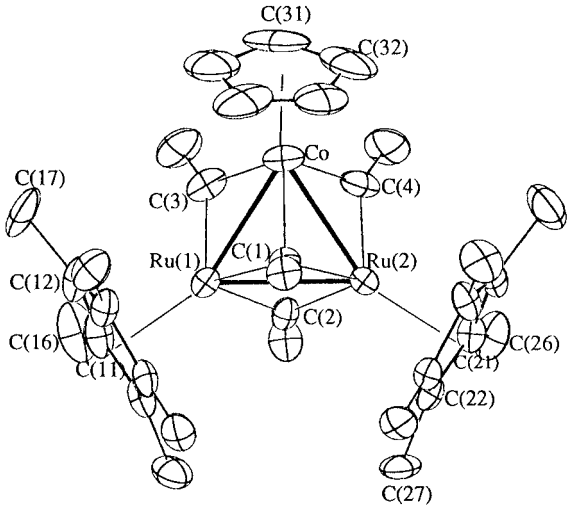

Figure 6. Molecular structure and numbering scheme for **8** drawn at the 30% probability level.

Table 7. Selected Bond Lengths (Å) and Angles (deg) for 8

Bond Lengths			
Ru(1)−Ru(1)	2.738(1)	Ru(1)−C(1)	2.069(10)
Ru(1)−Co	2.601(2)	Ru(1)−C(2)	2.043(9)
Ru(2)−Co	2.601(2)	Ru(1)−C(3)	1.953(10)
Ru(2)−C(1)	2.066(9)	Co−C(1)	2.091(9)
Ru(2)−C(2)	2.044(9)	Co−C(3)	1.998(11)
Ru(2)−C(4)	1.938(9)	Co−C(4)	1.979(11)
C(1)−O(1)	1.201(11)	C(2)−O(2)	1.174(11)
C(3)−O(3)	1.195(13)	C(4)−O(4)	1.186(13)

Bond Angles			
Ru(2)−Ru(1)−Co	58.26(4)	C(1)−Ru(1)−C(2)	96.1(4)
Ru(1)−Ru(2)−Co	58.23(4)	C(1)−Ru(1)−C(3)	101.3(4)
Ru(1)−Co−Ru(2)	63.51(4)	C(2)−Ru(1)−C(3)	83.9(4)
C(1)−Ru(2)−C(2)	96.1(4)	C(1)−Co−C(3)	99.0(4)
C(1)−Ru(2)−C(4)	100.8(4)	C(1)−Co−C(4)	98.5(4)
C(2)−Ru(2)−C(4)	83.5(4)	C(3)−Co−C(4)−	83.3(5)
Ru(1)−C(1)−Ru(2)	82.9(3)	Ru(1)−C(2)−Ru(2)	84.1(4)
Ru(1)−C(1)−Co	77.4(3)	Ru(1)−C(3)−Co	82.3(4)
Ru(2)−C(1)−Co	77.5(3)	Ru(2)−C(4)−Co	83.2(4)

Reaction of 2 with $CpCo(CO)_2$. The reaction between **2** and 2 equiv of $CpCo(CO)_2$ was carried out either photochemically (73% yield) or thermally (41% yield). The resulting dark red crystalline solid of the formula $(Cp^*Ru)_2(CpCo)(CO)_4$ (**8**) has four IR ν(CO) absorptions (Table 1) very similar to those of **5a** and **5b**. The X-ray diffraction analysis of **8** confirmed its structural similarity to **5a** (Figure 6 and Table 7) with the Ru−Ru−Co triangular metal frame capped by one CO and edge-bridged by three CO ligands. The Ru−Ru distance is longer in **8** (2.738(1) Å) than in **5a** (2.721-(3) Å).

Reaction of 2 with $[CpFe(CO)_2]_2$. A homometallic tetranuclear cluster of ruthenium, $(CpRu)_4(CO)_4$, has been reported to be formed in very low (3.4%) yield on thermolysis of the dimer $[CpRu(CO)_2]_2$ in boiling

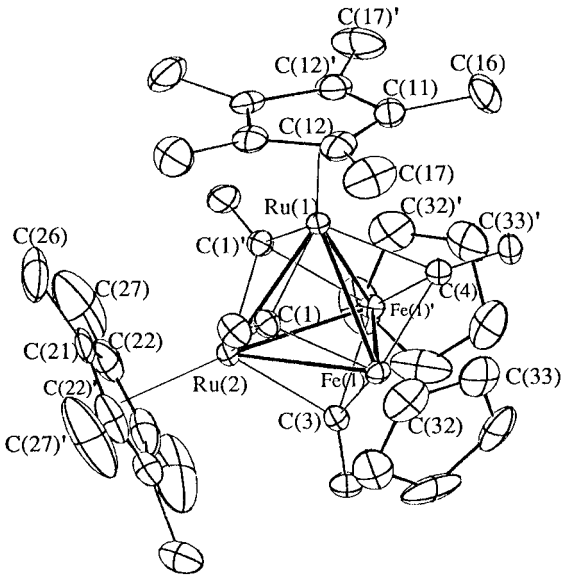

Figure 7. Molecular structure and numbering scheme for **9** drawn at the 30% probability level.

xylene for 4 weeks.[11] The complex has not been structurally characterized. The iron analog $(CpFe)_4(CO)_4$ has been prepared similarly, and the crystal structure has been analyzed.[12] An attempt to make mixed-metal clusters by refluxing equimolar amounts of $[CpRu(CO)_2]_2$ and $[CpFe(CO)_2]_2$ in xylene has resulted in a mixture of homometallic tetranuclear clusters in low yield.[11]

On irradiation of an equimolar mixture of **2** and $[CpFe(CO)_2]_2$ at room temperature for 40 h, and after workup on a column chromatograph, a dark green crystalline solid having the formula $(Cp^*Ru)_2(CpFe)_2(CO)_4$ (**9**) was obtained in 66% yield. The same compound was obtained in 41% yield when the initial mixture was heated at 60 °C for 72 h.

The structure of **9**, determined by single-crystal X-ray diffraction analysis, is shown in Figure 7, and its bond lengths and angles are given in Table 8. The molecule has a mirror plane that passes through two Ru atoms and the center of the Fe−Fe bond. The Fe−Fe distance (2.536(1) Å) is longer than that in $(CpFe)_4(CO)_4$ (2.520 Å (average)),[12] reflecting the existence of two Ru atoms in the tetrahedron of **9**. The triply bridging CO ligand coordinates to each plane of the tetrahedral metal framework. Though the molecule has two kinds of CO ligands, as evidenced by the X-ray structure and the ^{13}C NMR spectrum, the IR ν(CO) band was observed as a single absorption at 1634 cm^{-1} (Table 1). This is in contrast to the complicated ν(CO) bands in **6**, where the metal frame has a tetrahedral structure but is distorted due to unsaturation of the valence electrons.

Experimental Section

General Procedures. Most manipulations were performed under a dry oxygen-free argon atmosphere. Solvents were purified by standard methods and freshly distilled from Na−benzophenone or CaH_2 under argon before use. Photochemical reactions were performed with a Riko 100-W high-pressure mercury lamp in a Pyrex flask of 150 mL volume. The starting materials and complexes $Cp^*Rh(H)_2(SiEt_3)_2$,[13] $[Cp^*Ru]_2(\mu\text{-}H)_4$,[14] $[CpNi(CO)]_2$,[15] $[CpCo(NO)]_2$,[16] $[CpFe(CO)_2]_2$,[15] $[CpRu(CO)_2]_2$,[17] $[CpMo(CO)_2]_2$,[18] and $CpCo(CO)_2$[19] were obtained by published procedures. All other reagents were commercially obtained. ^1H and ^{13}C NMR spectra were measured on a JEOL EX-270 spectrometer, and IR spectra were recorded on a Perkin Elmer FT-1650 spectrometer using a CaF_2 liquid cell.

Table 8. Selected Bond Lengths (Å) and Angles (deg) for 9

Bond Lengths			
Ru(1)−Ru(2)	2.736(1)	Ru(2)−Fe(1)	2.627(1)
Ru(1)−Fe(1)	2.628(2)	Fe(1)−Fe(1)′	2.536(1)
Ru(1)−C(1)	2.086(8)	Ru(2)−C(1)	2.087(8)
Ru(1)−C(4)	2.093(11)	Ru(2)−C(3)	2.074(12)
Fe(1)−C(1)	2.045(8)	C(1)−O(1)	1.193(9)
Fe(1)−C(3)	1.996(10)	C(3)−O(3)	1.205(18)
Fe(13−C(4)	2.011 (9)	C(4)−O(4)	1.177(11)
Bond Angles			
Ru(2)−Ru(1)−Fe(1)	58.59(3)	Ru(1)−Ru(2)−Fe(1)	58.65(4)
Fe(1)−Ru(1)−Fe(1)′	57.69(4)	Fe(1)−Ru(2)−Fe(1)′	57.73(3)
Ru(1)−Fe(1)−Ru(2)	62.76(4)		
Ru(1)−Fe(1)−Fe(1)	61.16(4)		
Ru(2)−Fe(1)−Fe(1)′	61.14(3)		
C(1)−Ru(1)−C(1)′	97.3(3)	C(1)−Ru(2)−C(3)′	97.2(3)
C(1)−Ru(1)−C(4)	97.9(3)	C(1)−Ru(2)−C(3)	97.7(3)
C(1)−Fe(1)−C(3)	101.6(4)	Ru(1)−C(1)−Ru(2)	81.9(3)
C(1)−Fe(1)−C(4)	101.9(4)	Ru(1)−C(1)−Fe(1)	79.0(2)
C(3)−Fe(1)−C(4)	100.0(3)	Ru(2)−C(1)−Fe(1)	78.9(3)
Ru(2)−C(3)−Fe(1)	80.4(5)	Ru(1)−C(4)−Fe(1)	79.6(3)
Fe(1)−C(3)−Fe(1)	78.9(5)	Fe(1)−C(4)−Fe(1)′	78.2(4)

$(Cp^*Rh)(CpNi)_2(CO)_2$ (3). A mixture of $Cp^*Rh(H)_2(SiEt_3)_2$ (**1**; 94.1 mg, 0.2 mmol) and $[CpNi(CO)]_2$ (60.7 mg, 0.2 mmol) in THF (40 mL) was irradiated until most of **1** was consumed, as monitored by ^1H NMR spectra (4 days). The initially red solution became dark green, and a small quantity of dark red material precipitated. The solvent was evaporated under reduced pressure, and the residual dark green solid was chromatographed on alumina (deactivated with 5 wt % H_2O, 14 × 2 cm). Elution with hexane gave the starting material $Cp^*RhH_2(SiEt_3)_2$ (12.5 mg). The green solution eluted with hexane/CH_2Cl_2 (1/2) was collected and evaporated to dryness to yield the green crystalline solid of **3** (44.9 mg, 0.083 mmol, 41% yield). Anal. Calcd for $C_{22}H_{25}Ni_2O_2Rh$: C, 48.77; H, 4.65. Found: C, 48.52; H, 4.63. The X-ray sample was obtained by recrystallization from hexane as green plates.

Complex **3** was also obtained in 35% yield by heating a solution of **1** (37.7 mg, 0.08 mmol) and $[CpNi(CO)]_2$ (24.3 mg, 0.08 mmol) in toluene (10 mL) at 80 °C for 72 h followed by workup of the resulting solution as above.

$(Cp^*Rh)(CpCo)_2(NO)_2$ (4). A mixture of **1** (37.7 mg, 0.08 mmol) and $[CpCo(NO)]_2$ (24.6 mg, 0.08 mmol) in THF (40 mL) was irradiated for 62 h. The initially red solution became dark red. After the solvent was evaporated under reduced pressure, the residual dark red solid was chromatographed on alumina (deactivated with 5 wt % H_2O, 14 × 2 cm). Elution with hexane gave unreacted **1** (7.2 mg). The dark red solution eluted with CH_2Cl_2/THF (3/1) was collected and evaporated to dryness to yield the dark red crystalline solid of **4** (17.9 mg, 0.033 mmol, 41% yield). Anal. Calcd for $C_{20}H_{25}Co_2N_2O_2Rh$:

(11) Blackmore, T.; Cotton, J. D.; Bruce, M. I.; Stone, F. *G. A. J. Chem Soc. A* **1968**, 2931.
(12) Neuman, M. A.; T-Toan; Dahl, L. F. *J. Am. Chem. Soc.* **1972**, *94*, 3383.
(13) Fernandez, M.-J.; Bailey, P. M.; Bentz, P. O.; Ricci, J. C.; Koetzle, T. F.; Maitlis, P. M. *J. Am. Chem. Soc.* **1984**, *106*, 5458.
(14) Suzuki, H.; Omori, H.; Lee, D. H.; Yoshida, Y.; Fukushima, M.; Tanaka, M.; Moro-oka, *Y. Organometallics* **1994**, *13*, 1129.
(15) King, R. B. In *Organometallic Syntheses;* King, R. B., Ed.; Academic: New York, 1965; Vol. 1.
(16) Brunner, H. *J. Organomet. Chem.* **1968**, *12*, 517.
(17) Humphries, A. P.; Knox, S. A. R. *J. Chem. Soc., Dalton Trans.* **1975**, 1710.
(18) Curtis, M. D.; Hay, M. S. *Inorg. Synth.* **1990**, *28*, 150.
(19) Piper, T. S.; Cotton, F. A. J. *Inorg. Nucl. Chem.* **1955**, *1*, 313.

Table 9. Crystallographic Data for Complexes 3, 4, 5a, and 6

	$C_{22}H_{25}Ni_2O_2Rh$ (**3**)	$C_{20}H_{25}CO_2N_2O_2Rh$ (**4**)	$C_{24}H_{25}O_4RhRu_2$ (**5a**)	$C_{34}H_{40}Mo_2O_4Rh_2$ (**6**)
fw	541.8	546.2	682.5	910.4
cryst syst	monoclinic	monoclinic	orthorhombic	triclinic
space group	$P2_1/n$ (No. 14)	$P2_1/n$ (No. 14)	$Pna2_1$ (No. 33)	$P\bar{1}$ (No. 2)
a, Å	9.575(1)	13.424(1)	10.024 (1)	11.510(2)
b, Å	10.311(1)	11.473(1)	14.147(1)	11.864(5)
c, Å	21.625(1)	14.029(1)	15.985 (1)	23.445(5)
α, deg				87.81(3)
β, deg	96.80(1)	107.905(8)		88.92(2)
γ, deg				87.14(3)
V, Å^3	2111.0(2)	2055.8(2)	2266.8(2)	3195(2)
Z	4	4	4	4
cryst size, mm	0.40 × 0.32 × 0.19	0.48 × 0.25 × 0.17	0.24 × 0.23 × 0.11	0.23 × 0.18 × 0.11
color	green	dark red	green	dark red
d_{calc}, g cm^{-3}	1.705	1.765	2.000	1.893
μ, cm^{-1}	25.5	23.9	20.3	17.9
2θ scan range, deg	4.0−55.0	4.0−55.0	4.0−55.0	4.0−50.0
data collected (h,k,l)	+12,+13,±28	+17,−14,±18	+12,−18,−20	+13,±14,±27
no. of unique rflns ($F_o \geq 4\sigma(F_o)$)	3180	3038	2040	6111 ($F_o \geq 3\sigma(F_o)$)
no. of params refined	245	245	281	758
R	0.042	0.045	0.031	0.081
R_w	0.047	0.051	0.037	0.083

Table 10. Crystallographic Data for Complexes 7−9

	$C_{32}H_{40}Ni_2O_2Ru_2$ (**7**)	$C_{25}H_{35}CoO_4Ru_2$ (**8**)	$C_{34}H_{40}Fe_2O_4Ru_2$ (**9**)
fw	776.2	708.7	826.5
cryst syst	triclinic	tetragonal	hexagonal
space group	$P\bar{1}$ (No. 2)	$P4_12_12$ (No. 92)	$P6_3/m$ (No. 176)
a, Å	11.104(1)	15.978(1)	18.202(1)
b, Å	16.179(1)		
c, Å	26.193(2)	21.594(1)	16.109(1)
α, deg	84.260(5)		
β, deg	86.143(5)		
γ, deg	85.691(5)		
V, Å^3	4660.3(4)	5514.3(5)	4622.1(3)
Z	6	8	6
cryst size, mm	0.43 × 0.14 × 0.10	0.33 × 0.17 × 0.12	0.34 × 0.21 × 0.17
color	dark red	dark red	green
d_{calc}, g cm^{-3}	1.660	1.707	1.782
μ, cm^{-1}	21.6	16.9	19.0
2θ scan range, deg	4.0−55.0	4.0−55.0	4.0−55.0
data collected (h,k,l)	−14,±20,±33	−20,±20,+28	+23,±23,−20
no. of unique rflns ($F_o \geq 4\sigma(F_o)$)	12 532	3000	2559
no. of params refined	1028	326	206
R	0.046	0.042	0.043
R_w	0.053	0.050	0.052

C, 43.98; H, 4.61; N, 5.86. Found: C, 43.52; H, 4.63; N, 5.53. Single crystals were obtained by recrystallization from hexane as dark red plates.

Complex **4** was also obtained in 86% yield by the thermal reaction of **1** (37.7 mg, 0.08 mmol) with $[CpCo(NO)]_2$ (24.6 mg, 0.08 mmol) in toluene (10 mL) at 70 °C for 48 h.

(Cp*Rh)(CpRu)$_2$(CO)$_4$ (5a). A mixture of **1** (37.7 mg, 0.08 mmol) and $[CpRu(CO)_2]_2$ (35.8 mg, 0.08 mmol) in toluene (10 mL) was heated at 70 °C for 48 h. The initially yellow solution became dark red while a small quantity of dark red material precipitated. The solvent was evaporated under reduced pressure, and the residual dark red solid was chromatographed on alumina (deactivated with 5 wt % H_2O, 14 × 2 cm). Elution with hexane gave unreacted **1** (5.7 mg). The green solution eluted with hexane/CH_2Cl_2 (1/1) was collected and evaporated to dryness to yield the green crystalline solid of **5a** (20.7 mg, 0.03 mmol, 38% yield). It was recrystallized from toluene to give single crystals as green plates. Anal. Calcd for $C_{24}H_{25}O_4RhRu_2$: C, 42.24; H, 3.69. Found: C, 42.55; H, 3.47.

(Cp*Rh)(CpFe)$_2$(CO)$_4$ (5b). A mixture of **1** (37.7 mg, 0.08 mmol) and $[CpFe(CO)_2]_2$ (28.3 mg, 0.08 mmol) in toluene (10 mL) was heated at 70 °C for 72 h. The initially yellow solution became dark red, and a small quantity of dark red material precipitated. After the solvent was evaporated under reduced pressure, the residual dark red solid was chromatographed on alumina (deactivated with 5 wt % H_2O, 14 × 2 cm). Elution with hexane gave recovered **1** (3.3 mg). The red solution eluted with CH_2Cl_2 was collected and evaporated to dryness to yield the dark red crystalline solid of **5b** (24.9 mg, 0.042 mmol, 53% yield). Anal. Calcd for $C_{24}H_{25}Fe_2O_4Rh$: C, 48.69; H, 4.26. Found: C, 48.25; H, 4.31.

(Cp*Rh)$_2$(CpMo)$_2$(CO)$_4$ (6). A mixture of **1** (75.3 mg, 0.16 mmol) and $[CpMo(CO)_2]_2$ (34.7 mg, 0.08 mmol) in THF (40 mL) was irradiated until most of complex **1** was consumed (ca. 62 h), as monitored by ^{1}H NMR spectra. The initially red solution became dark red while a small quantity of dark red material precipitated. The solvent was evaporated under reduced pressure, and the residual dark red solid was chromatographed on alumina (deactivated with 5 wt % H_2O, 14 × 2 cm). Elution with hexane gave the recovered **1** (13.3 mg). The dark red solution eluted with CH_2Cl_2 was collected and evaporated to dryness to yield the dark red crystalline solid of **6** (17.9 mg, 0.019 mmol, 24% yield). Anal. Calcd for $C_{34}H_{40}Mo_2O_4Rh_2$: C, 44.86; H, 4.43. Found: C, 44.63; H, 4.34. Single crystals were obtained by recrystallization from toluene as dark red plates.

Complex **4** was obtained by a thermal reaction in better yield. A mixture of **1** (75.3 mg, 0.16 mmol) and $[CpMo(CO)_2]_2$ (34.7 mg, 0.08 mmol) in toluene (10 mL) was heated to 70 °C for 70 h to give **4** in 58% yield.

(Cp*Ru)$_2$(CpNi)$_2$(CO)$_2$ (7). A solution of $(Cp^*Ru)_2(\mu\text{-}H)_4$ (**2**; 38.1 mg, 0.08 mmol) and $[CpNi(CO)]_2$ (24.3 mg, 0.08 mmol) in THF (40 mL) was irradiated at room temperature for 24 h.

The initially red solution became dark green while a small quantity of black material precipitated. The solvent was evaporated under reduced pressure, and the residual dark green solid was chromatographed on alumina (deactivated with 5 wt % H_2O, 10 × 2 cm). The dark red solution eluted with hexane/CH_2Cl_2 (3/1) was collected and evaporated to dryness to yield thje dark red crystalline solid of **7** (22.4 mg, 0.029 mmol, 36% yield). Anal. Calcd for $C_{32}H_{40}Ni_2O_2Ru_2$: C, 49.52; H, 5.19. Found: C, 49.91; H, 5.11. Single crystals were obtained by recrystallization from hexane as dark red plates.

$(Cp^*Ru)_2(CpCo)(CO)_4$ (8). A mixture of **2** (38.1 mg, 0.08 mmol) and $CpCo(CO)_2$ (28.8 mg, 0.16 mmol) in THF (40 mL) was irradiated until most of **2** was consumed (ca. 48 h), as monitored by ^{1}H NMR spectra. The initially red solution became dark, and a small quantity of dark red material precipitated. The solvent was evaporated under reduced pressure. The residual dark red solid was chromatographed on alumina (deactivated with 5 wt % H_2O, 14 × 2 cm). Elution with hexane/CH_2Cl_2 (1/1) gave a dark red band. The dark red solution eluted was collected and evaporated to dryness to yield the dark red crystalline solid of **8** (41.5 mg, 0.058 mmol, 73% yield). Anal. Calcd for $C_{29}H_{35}CoO_4Ru_2$: C, 49.15; H, 4.98. Found: C, 48.68; H, 5.19. Single crystals were obtained by recrystallization from hexane as dark red cubes.

Complex **8** was also obtained by heating a mixture of **2** (38.1 mg, 0.08 mmol) and $CpCo(CO)_2$ (28.8 mg, 0.16 mmol) in toluene (10 mL) at 60 °C for 72 h in a yield of 41%.

$(Cp^*Ru)_2(CpFe)_2(CO)_4$ (9). A mixture of **2** (38.1 mg, 0.08 mmol) and $[CpFe(CO)_2]_2$ (28.3 mg, 0.08 mmol) in THF (40 mL) was irradiated at room temperature. The initially red solution became dark green while a small quantity of dark red material precipitated. After 40 h, the solvent was evaporated under reduced pressure. The residual dark green solid was chromatographed on alumina (deactivated with 5 wt % H_2O, 13 × 2 cm). Elution with CH_2Cl_2 gave a dark green band. The dark green solution eluted was collected and evaporated to dryness to yield the dark green crystalline solid of **9** (43.6 mg, 0.06 mmol, 66% yield). Anal. Calcd for $C_{34}H_{40}Fe_2O_4Ru_2$: C, 49.41; H, 4.88. Found: C, 49.40; H, 4.92. Single crystals were obtained by recrystallization from toluene as dark green pillars.

Thermal reaction was carried out by heating a mixture of **2** (71.5 mg, 0.15 mmol) and $[CpFe(CO)_2]_2$ (53.1 mg, 0.15 mmol) in toluene (10 mL) at 60 °C for 72 h to give **9** in 41% yield.

X-ray Crystallographic Analysis. Crystal, data collection, and refinement parameters are summarized in Tables 9 and 10. Reflection data were collected at room temperature on an Enraf-Nonius CAD-4 diffractometer using graphite-monochromated Mo Kα (λ = 0.710 73 Å) radiation and the $\omega-2\theta$ scan technique. The intensity data were corrected for absorption anisotropy effects. The structures were solved from direct and Fourier methods and refined by block-diagonal least squares with anisotropic thermal parameters in the last cycles for all non-hydrogen atoms. Hydrogen atoms were not located. The function minimized in the least-squares refinement was $\sum w(|F_o| - |F_c|)^2$. In the asymmetric unit of **4** and **5a**, there were two and three independent molecules, respectively. The computational program package used in the analysis was UNICS-III program system.[20] Neutral atomic scattering factors were taken from ref 21. Important bond lengths and angles are given in Tables 2−8.

Acknowledgment. T.N. acknowledges the research fellowship of the Japan Society for the Promotion of Science for Young Scientists.

Supporting Information Available: Tables of positional and thermal parameters and bond lengths and angles for **3**, **4**, **5a**, and **6**−**9** (43 pages). Ordering information is given on any current masthead page.

OM970772C

(20) Sakurai, T.; Kobayashi, K. *Rikagaku Kenkyuusho Hokoku* **1979**, *55*, 69.

(21) *International Tables for X-Ray Crystallography;* Kynoch: Birmingham, England, 1974; Vol. IV.